Available online at www.sciencedirect.com
ScienceDirect
Journal of Organometallic Chemistry 692 (2007) 4093–4105
Journal of Organometallic Chemistry
www.elsevier.com/locate/jorganchem

The 3,5-dimethyl-4-nitropyrazole ligand in the construction of supramolecular networks of silver(I) complexes

Paloma Ovejero [a], M. José Mayoral [a], Mercedes Cano [a,*], José A. Campo [a], José V. Heras [a], Elena Pinilla [a,b], M. Rosario Torres [b]

[a] *Departamento de Química Inorgánica I, Facultad de Ciencias Químicas, Universidad Complutense, 28040 Madrid, Spain*
[b] *Laboratorio de Difracción de Rayos-X, Facultad de Ciencias Químicas, Universidad Complutense, 28040 Madrid, Spain*

Received 13 April 2007; received in revised form 5 June 2007; accepted 7 June 2007
Available online 21 June 2007

Abstract

Three new ionic silver complexes based on the 3,5-dimethyl-4-nitropyrazole ligand (Hpz^{NO_2}) and 1:2 or 1:3 (Ag : Hpz^{NO_2}) stoichiometries, $[Ag(Hpz^{NO_2})_2][BF_4]$, $[Ag(Hpz^{NO_2})_3][SbF_6]$ and $[Ag(Hpz^{NO_2})_3]$ $[PO_2F_2] \cdot Hpz^{NO_2}$ have been prepared and structurally characterised. The linear or trigonal metallic coordination environment, the NO_2 groups on the pyrazole ligand as well as the presence of counteranions of the type AX_n^-as BF_4^-, SbF_6^- or PF_6^- (the latter one evolving to $PO_2F_2^-$) were strategically selected to produce molecular assemblies established on the basis of hydrogen-bonds (N–H···X) and π···π or coordinative interactions involving the NO_2 group. The complex $[Ag(Hpz^{NO_2})_2][BF_4]$ exhibited polymeric N–H···F hydrogen-bonded chains which were assembled in a 3D network by weaker coordinative Ag···O(NO_2) and π(NO_2)···π(NO_2) interactions. In the complex $[Ag(Hpz^{NO_2})_3][SbF_6]$, consistent with the three-coordinated molecular environment, the interactions were extended to give rise an open 3D cationic sub-network in which the counteranions SbF_6^- were encapsulated. By contrast, in the related complex $[Ag(Hpz^{NO_2})_3]$ $[PO_2F_2] \cdot Hpz^{NO_2}$ the presence of a fourth non-coordinated pyrazole Hpz^{NO_2} avoided the formation of a 3D network giving rise to a double-chained 1D structure.

Keywords: Supramolecular arrays; Silver complexes; 3,5-Dimethyl-4-nitropyrazole; Hydrogen-bonds

1. Introduction

The design of new materials with predictable structures and properties, main goal of crystal engineering, is an increasing area of current research due its multidisciplinary incidence in different areas as materials chemistry, supramolecular chemistry or biology. In this context, the knowledge of the molecular arrangement in the crystal network as responsible for the properties of the material is of capital importance, the intermolecular interactions being the main tool to achieve the required packing for selected properties.

Among the intermolecular interactions, strong hydrogen-bonds and coordinative bonds have been mainly developed for a wide variety of supramolecular 1D, 2D and 3D architectures based on 0D coordination compounds [1,2], or for multifunctional compounds [3].

However, in order to complete the crystal engineering studies the presence of other weaker interactions as π···π interactions or non-conventional hydrogen-bonds are more and more recognised in building new interesting supramolecular architectures [4].

Previous works in our lab have been dealt with the study of the molecular assembly of several ionic metal complexes based on substituted pyrazole ligands, in which the hydrogen-bonds between the counteranion and the NH-pyrazole groups were the main tool for the molecular assembly [5–8], although some other factors as variations of the counteranion and substituents on the pyrazole ligands also drove the supramolecular arrangement.

* Corresponding author. Fax: +34 91 3944352.
E-mail address: mmcano@quim.ucm.es (M. Cano).

0022-328X/$ - see front matter © 2007 Elsevier B.V. All rights reserved.
doi:10.1016/j.jorganchem.2007.06.015

In this work, we extend the potentiality of new ionic silver complexes based on the 3,5-dimethyl-4-nitropyrazole (Hpz^{NO_2}) ligand for a rational design of extended hydrogen-bonding polymers or supramolecular arrays established on coordinative, π···π and/or non-conventional hydrogen-bond interactions. The influence of a *cis* or *trans* molecular geometry, the nature of the counteranion (geometry and coordinative ability), the presence of the NO_2 group on the pyrazole ligands and the molecular stereochemistry are the factors examined on the final 1D, 2D or 3D architectures.

2. Results and discussion

2.1. Structural comparative study of ionic silver complexes based on pyrazole-type ligands

In order to analyse the main factors which can control the molecular assembly of ionic silver(I) pyrazole-based complexes, a comparative study of the previous structural results of those of the type $[Ag(Hpz^*)_2][AX_n]$ (Hpz^* = substituted pyrazole ligand; AX_n = counteranion) is considered here as potential support for predictable structures of new derivatives. Following the literature data and our own research results [6,8–10], we have found in all cases a linear N–Ag–N coordination with a *cis*, *trans* or intermediate *cis–trans* orientation of the two NH groups from the two pyrazole ligands (deduced from the torsion angle τ defined by the four nitrogens of the two pyrazoles [8]), which is determinant of the supramolecular assembly. In particular, in the complex *cis*-$[Ag(Hpz^{bp_2})_2][BF_4]$ (**1**) (Hpz^{bp_2} = 3,5-di(*p*-butoxyphenyl)pyrazole) both pyrazole ligands are hydrogen-bonded to the same counteranion BF_4^- giving rise to closed molecular unities, which are bonded through additional weaker intermolecular C–H···F contacts in a 1D framework (Fig. 1a) [6,8]. By contrast, in the related complex *trans*-$[Ag(Hpz^{Me_2})_2][NO_3]$ (**2**) (Hpz^{Me_2} = 3,5-dimethylpyrazole) the cationic units are linked by bridging NO_3^- groups in a zig-zag polymeric 1D chain involving strong N–H···O hydrogen-bonds (Fig. 1b) [10]. Those structural results suggest that bulky substituents on the pyrazole group appear to prevent the formation of polymeric hydrogen-bonded chains based on the *trans*-oriented pyrazole groups. However, it was not at all true.

So, the complex $[Ag(Hpz^{NO_2})_2][CF_3SO_3]$ (**3**) where Hpz^{NO_2} is 3,5-dimethyl-4-nitropyrazole (this ligand having the same CH_3 substituents at the 3 and 5 positions of the ring as they are in **2**) surprisingly exhibits a *cis* orientation ($\tau = 2.0°$), from which cyclic unities with the corresponding counteranion are formed (Fig. 1c) [6,8]. The cyclic molecular entities are linked in dimers (by strong coordinative

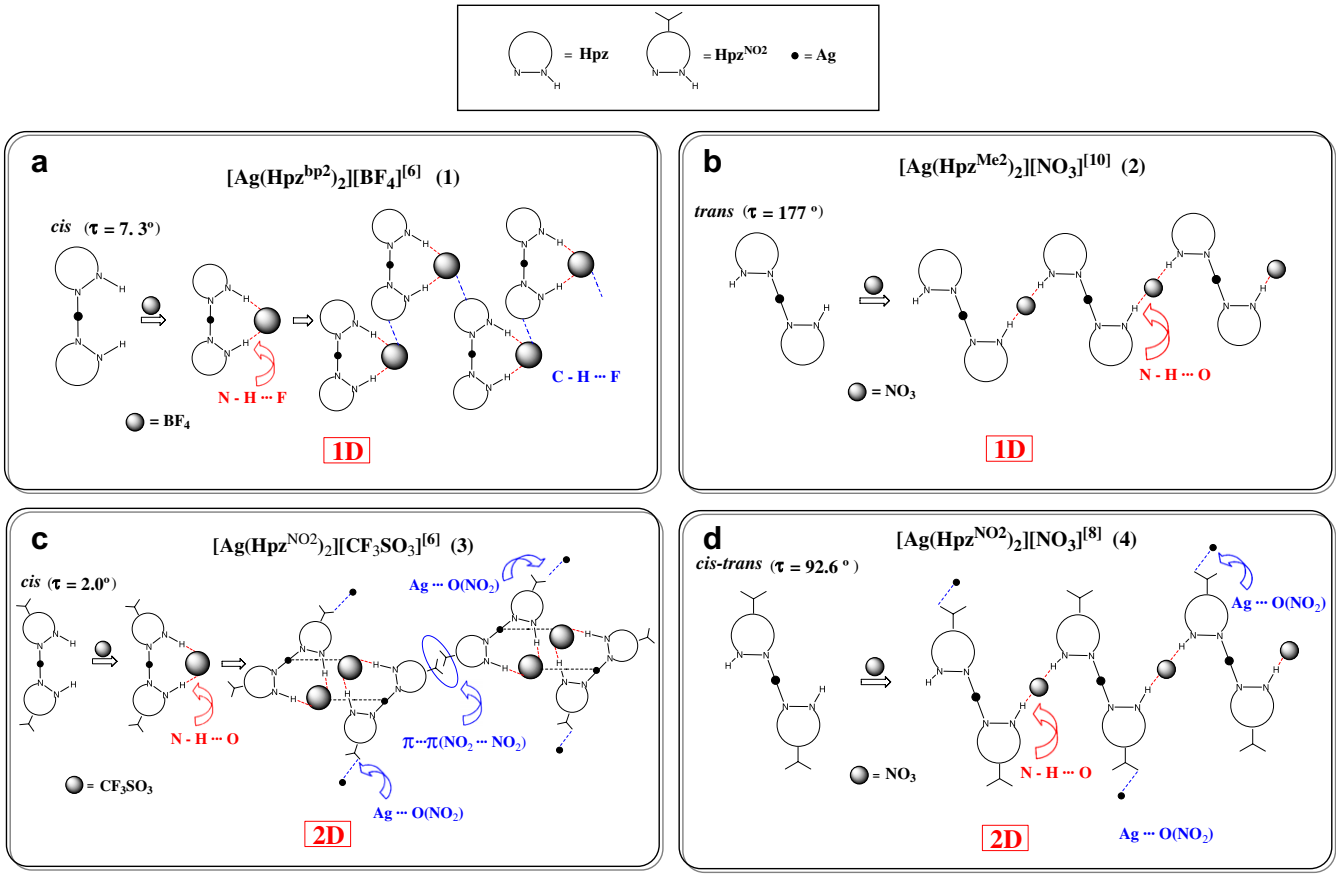

Fig. 1. Schematic representation of the molecular assemblies of complexes **1**–**4** ((a)–(d), respectively).

Ag···O interactions involving the $CFSO_3^-$ counteranion), and these dimers assembled in columns by π···π (NO_2···NO_2) contacts (Fig. 1c). Subsequent coordinative Ag···O intercolumnar interactions (also involving the NO_2 groups) give rise to a 2D layer-like framework (Fig. 1c) [6].

The crystal structure of the related complex $[Ag(Hpz^{NO_2})_2][NO_3]$ (**4**) shows an intermediate *cis–trans* (pyrazole to pyrazole) orientation ($\tau = 92.6°$), which also produces a polymeric 1D chain acting the counteranion NO_3^- as bridge (Fig. 1d) [8]. Additional Ag···O interactions from the NO_2 substituents are the support of a 2D layer-like network (Fig. 1d).

Fig. 1 depicts a schematic representation of the structural results of this family of compounds.

As main result of the comparative structural analysis of **1**–**4** (Fig. 1) it can be established that contributions of substituents at the pyrazole ligand as well as the counteranions are determinant of the supramolecular organisation of ionic metal complexes $[Ag(Hpz^*)_2][AX_n]$. Therefore, factors such as the size, geometry and coordinative ability of the counteranions, or the presence of coordinative groups on the ligand, should be conveniently selected in designing supramolecular networks.

Considering the results previously described, the NO_2 substituent at the 4 position of the ring can be useful to produce hydrogen-bonding and/or coordinative or π···π interactions (Fig. 2) [8]. Therefore we consider the Hpz^{NO_2} ligand to be adequate to perform two- or three-dimensional networks of complexes $[Ag(Hpz^{NO_2})_2][AX_n]$ specially if they exhibit a *trans* or *cis–trans* intermediate orientations of the pyrazole ligands, as we have above described. On the other hand, because of the coordinative sterically demanding anion $CF_3SO_3^-$ gave rise to the *cis*-complex **3** [6], the smaller tetrahedral counteranion BF_4^- having low coordinative ability is suggested as candidate to produce the desired *trans* orientation of the pyrazole groups.

With these considerations in mind and in order to confirm the above proposal, in this work the complex $[Ag(Hpz^{NO_2})_2][BF_4]$ (**5**) has been prepared and its crystalline structure is reported. In fact, the complex exhibits the expected *trans* geometry which supports a 3D supramolecular network, as described below.

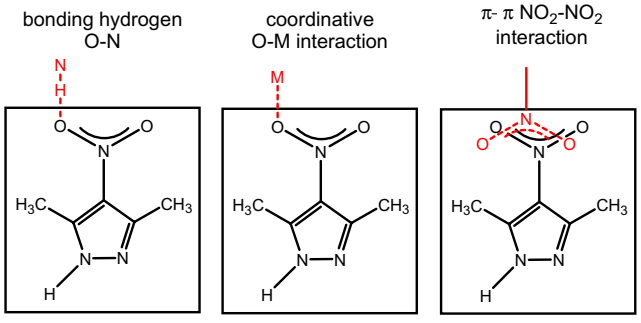

Fig. 2. Schematic representation of the potential interactions through the NO_2 group of the Hpz^{NO_2} ligand.

On the other hand, on the basis of the well-established three-coordinated azolyl–silver complexes [11], new trigonal silver(I) derivatives containing a 1:3 (Ag : Hpz^{NO_2}) stoichiometry can be proposed as support of acentric arrangements, useful for non-linear optical properties [12]. Following these considerations, the silver salts $AgSbF_6$ and $AgPF_6$ were allowed to react with the Hpz^{NO_2} ligand in a 1:3 molar ratio. From these reactions, the complexes $[Ag(Hpz^{NO_2})_3][SbF_6]$ (**6**) and $[Ag(Hpz^{NO_2})_3][PO_2F_2]\cdot Hpz^{NO_2}$ (**7**) were isolated, and their crystal structures solved and reported in this work.

2.2. Synthetic and characterisation studies

Compounds **5**–**7** were prepared by reaction of the corresponding silver salt with the pyrazole Hpz^{NO_2} ligand in a 1:2 or 1:3 molar ratio. The reactions were carried out in the darkness due to partial decomposition of the compounds when we were light-exposed.

All complexes were air-stable white solids. They were characterised by analytical and spectroscopic techniques (IR and ^1H NMR), and all data agree with their proposed molecular formulation. ^{31}P NMR spectroscopy was also used for complex **7**. All data are listed in Section 3.

The IR spectra show, amongst others, the characteristic bands of the pyrazole ligands and those from the corresponding counteranions [5–7,13–15]. As general pattern, it is observed an absorption band at ca. 1600 cm^{-1} associated to the typical ν(C–N) + ν(C–C) vibrations and a multiple and intense absorption in the 3300–2700 cm^{-1} interval from the ν(NH) and ν(CH) vibrations. The latter frequencies are similar to those of the free ligand which exhibits strong hydrogen-bonds [16], suggesting the presence of such interactions in our compounds.

The ^1H NMR spectra in $CDCl_3$ solution at room temperature show in all cases only a singlet corresponding to the CH_3 protons, indicating the equivalence of all the methyl groups. Thus, it is possible to suggest a metallotropic equilibrium to explain the above behaviour similar to that previously found for related complexes [6,17]. This equilibrium could be responsible for the absence of signals attributed to the NH protons. An alternative explanation emerges by considering the hydrogen-bonds as determinant factor of the absence of NH resonances. So, new ^1H NMR experiments in highly diluted solutions in the temperature range of 5–50 °C allowed us to observe the NH signal at 11.78 ppm for compound **5**, but not for **6**, this different behaviour being attributed to their different structural characteristics.

It is interesting to mention that, although the synthetic procedure of compound **7** was carried out by reaction between $AgPF_6$ and Hpz^{NO_2} in a 1:3 molar ratio, the new compound exhibits an unexpected formulation involving four pyrazole ligands each metal as well as $PO_2F_2^-$ as counteranion. The presence of $PO_2F_2^-$ was confirmed by the triplet signal at −15.5 ppm observed in the $^{31}P\{^1H\}$ NMR spectrum of **7**. The transformation of PF_6^- to

$PO_2F_2^-$ occurs through a hydrolysis process which has already been observed in some examples described in the literature [14,18]. The fourth pyrazole ligand was proved to be non-coordinated, acting as a crystallisation molecule.

Adequate single crystals for X-ray purposes were obtained for the three compounds, confirming the formulation proposed.

2.3. Crystal structure of $[Ag(Hpz^{NO_2})_2][BF_4]$ (5)

The X-ray crystal structure of **5** is depicted in Fig. 3, and Table 1 lists selected bond distances and angles. Table 2 shows hydrogen-bond geometries. The compound crystallises in the monoclinic system, space group $P2_1/c$. The asymmetric unit consists of a cationic unit $[Ag(Hpz^{NO_2})_2]^+$ held by a moderate bifurcated hydrogen-bond to the BF_4^- counteranion involving one of the NH-pyrazolic group and the F1 and F4 atoms (Table 2). The Ag–N distances are similar to other observed in related compounds containing heterocyclic ligands [6,9,10,19]. The N1–Ag–N4 angle of 169.3(2)° agrees with the typical linear coordination around the silver centre.

The NO_2 planes are almost coplanar with the own pyrazole planes (dihedral angles of 4.8(2)° and 5.9(4)°). Besides, the pyrazole rings are also coplanar between them (dihedral angle of 6.5(2)°), indicating the planarity of the whole cationic entity.

The pyrazole ligands exhibit a *trans* orientation of the NH groups, as deduced by the torsion angle τ defined by the four nitrogen atoms of 177.1(4)°, which in agreement with our hypothesis should favour the polymeric chain ordering. In fact, the BF_4^- counteranion is bonded through a moderate hydrogen-bond between the F2 atom and the NH group of the neighbouring cationic unit (Table 2), giving rise to a zig-zag polymeric chain which lies parallel to the *a* axis (Fig. 4a). In this distribution the cationic unit is twisted an angle of 25.6(1)° with respect to the *ab* plane. All the hydrogen-bond interactions produce an approach of the silver centre to fluorine atoms of the closest counteranions with Ag···F distances in the range of 3.0–3.5 Å (Ag···F4 3.043(4) Å; Ag···F2 $(x-1, y, z)$ 3.437(4) Å), which also support the 1D distribution.

The chains are further extended to a 2D arrangement through coordinative Ag···O interactions with the oxygen atoms of the NO_2 groups (Ag···O4 $(-x+1, y+1/2, -z+1/2)$ 2.815(4) Å; Ag···O3 $(-x+1, y+1/2, -z+1/2)$ 3.041(4) Å), so generating a corrugated layer in the *ab* plane (Fig. 4b).

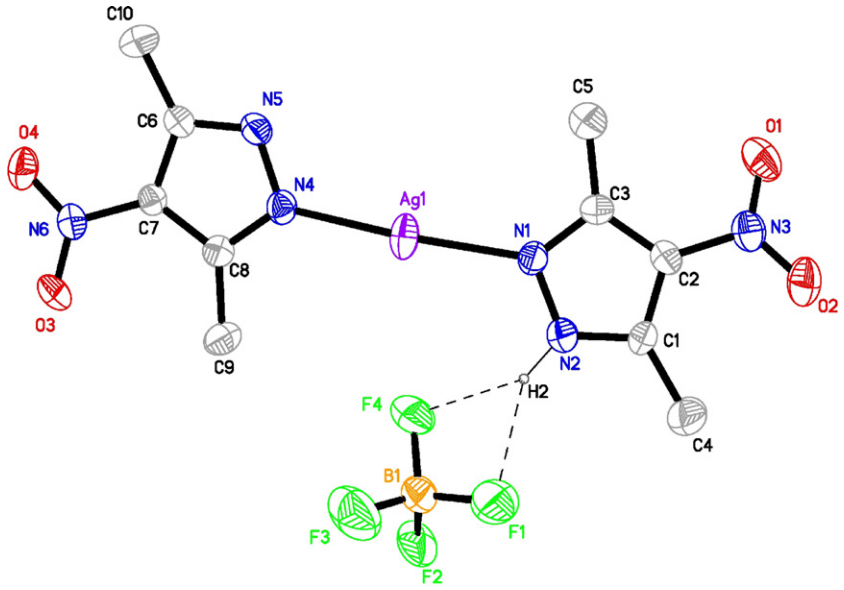

Fig. 3. A ORTEP view of $[Ag(Hpz^{NO_2})_2][BF_4]$ (**5**), showing the numbering atom. Hydrogen atoms, except H2, have been omitted for clarity. The thermal ellipsoids are at 40% probability level.

Table 1
Bond lengths (Å) and angles (°) for **5**–**7**

	$[Ag(Hpz^{NO_2})_2][BF_4]$ (**5**)	$[Ag(Hpz^{NO_2})_3][SbF_6]$ (**6**)	$[Ag(Hpz^{NO_2})_3][PO_2F_2]\cdot Hpz^{NO_2}$ (**7**)
Ag–N1	2.155(4)	2.272(8)	2.218(5)
Ag–N4	2.135(4)	2.249(9)	2.207(5)
Ag–N7		2.243(8)	2.322(6)
N1–Ag–N4	169.3(2)	111.5(3)	139.6(2)
N1–Ag–N7		118.4(3)	108.0(2)
N4–Ag–N7		129.0(3)	109.8(2)

Table 2
Hydrogen-bond geometries of **5**–**7**

D–H···A	*d*(D–H) [Å]	*d*(H···A) [Å]	*d*(D···A) [Å]	∠(D–H···A) [°]
$[Ag(Hpz^{NO_2})_2][BF_4]$ (**5**)				
N2–H2···F1	0.99	2.19	2.978(6)	135.5
N2–H2···F4	0.99	1.98	2.873(5)	149.2
N5–H5···F2[a]	0.98	1.85	2.766(5)	154.1
N5–H5···F3[a]	0.98	2.49	3.297(6)	138.6
$[Ag(Hpz^{NO_2})_3][SbF_6]$ (**6**)				
N8–H8···F5	0.95	2.26	3.15(2)	156.6
N8–H8···O3[b]	0.95	2.51	3.10(1)	120.5
N2–H2···O6[c]	1.05	1.95	2.99(1)	168.1
N5–H5···O1[d]	1.03	1.98	2.98(1)	165.9
N2–H2···F6[e]	1.05	2.64	3.13(2)	107.9
$[Ag(Hpz^{NO_2})_3][PO_2F_2]\cdot Hpz^{NO_2}$ (**7**)				
N2–H2···O9	0.93	2.21	2.88(1)	128.8
N8–H8···N11	0.99	1.92	2.848(8)	156.0
N8–H8···N10	0.99	2.62	3.334(8)	129.5
N10–H10···O10[f]	0.99	1.85	2.829(8)	170.5
N5–H5···O10[f]	0.96	1.82	2.777(7)	178.1
N2–H2···O5[g]	0.93	2.35	3.093(9)	137.5

[a] $x-1, y, z$.
[b] $-x+1/2, y+1/2, z$.
[c] $x-1/2, -y+3/2, -z+1$.
[d] $x, -y+3/2, z+1/2$.
[e] $-x+1/2, y-1/2, z$.
[f] $x+1, y, z$.
[g] $-x+1, -y, -z+1$.

Additional π···π interactions between NO_2 groups of consecutive layers (which have not been implicated in the above Ag···O interactions) (N3···N3 $(-x+1, -y+1, -z)$ 3.147(6) Å; O2···N3 $(-x+1, -y+1, -z)$ 3.233(6) Å; O1···O2 $(-x+1, -y+1, -z)$ 3.416(6) Å) extends the supramolecular dimensionality to a 3D network (Fig. 4c). Similar π···π (NO_2···NO_2) interactions have been reported for other compounds [6,20].

From a point of view of topology, the structure could be visualized as layers of cationic entities with the BF_4^- counteranions occupying the interlayer spacing (Fig. 5).

2.4. Crystal structure of $[Ag(Hpz^{NO_2})_3][SbF_6]$ (6)

The X-ray crystal structure of **6** is depicted in Fig. 6 and Tables 1 and 2 list selected distances and angles. The compound crystallises in the orthorhombic system, space group *Pbca*. The asymmetric unit consists of a cationic unit held by a hydrogen-bond to the SbF_6^- counteranion (Table 2). The silver centre is three-coordinated to three pyrazole ligands by their corresponding pyridinic N-atoms, and deviated 0.137(1) Å from the plane defined for these nitrogen atoms N1, N4 and N7. The Ag–N distances of ca. 2.25 Å (Table 1) are in the range found for related examples [6,9–11b,19,21]. However they are slightly longer than those observed in **5**, this fact being attributed to the crowding imposed by the coordination of three pyrazole ligands. The N–Ag–N angles (Table 1; mean value of 119.6(3)°) are consistent with the presence of a pseudo-C_3 axis passing through the silver centre. The relative orientation of the pyrazole ligands are also in agreement with this pseudo-axis, exhibiting dihedral angles between pyrazole planes of 55.9(4)°, 64.4(4)° and 76.7(4)°. The NO_2 planes are almost coplanar with the own pyrazole planes (dihedral angles of 4(1)°, 4.8(5)° and 7.6(5)°).

The supramolecular arrangement of this compound is dominated by moderate hydrogen-bonds from the NO_2 substituents and the NH groups of pyrazole ligands of neighbouring cationic unities (Table 2). Through these hydrogen-bonds, an open 3D cationic sub-network with channels along the *a* axis is generated, the cavities within the channels being formed by six cationic units (Fig. 7). Then, taking the silver centres as reference, a honey-comb type structure can be described (Fig. 7). The channels are occupied by the SBF_6^- counteranions (Fig. 8), which are linked by coordinative Ag···F1 $(-x+1, y-1/2, -z+1/2)$ interaction of 2.87(1) Å and bifucarted hydrogen-bonds (Table 2) to the cationic units. Both kind of interactions support the building of an open network with the SbF_6^- anion acting as template. The role of anions as template in supramolecular chemistry has recently been revised [22].

2.5. Crystal structure of $[Ag(Hpz^{NO_2})_3][PO_2F_2]\cdot Hpz^{NO_2}$ (7)

Looking for new open supramolecular structures like that observed in **6**, we tried to prepare similar compounds varying the counteranion. So, we carried out the reaction between $AgPF_6$ and Hpz^{NO_2} in a 1:3 stoichiometric molar ratio. Surprisingly the isolated compound presented the formulation $[Ag(Hpz^{NO_2})_3][PO_2F_2]\cdot Hpz^{NO_2}$ (**7**), which could be explained by considering a hydrolysis process of the anion PF_6^- to give $PO_2F_2^-$. The new compound **7**, exhibiting the expected three pyrazole ligands coordinated to the metal centre, has an additional non-coordinated pyrazole group Hpz^{NO_2} as a crystallisation molecule, which drastically modify the supramolecular network observed in **6**.

Fig. 9 shows a ORTEP representation of the asymmetric unit of **7**, and Tables 1 and 2 present selected distances and angles. The compound crystallises in the monoclinic system, space group $P2_1/c$.

The asymmetric unit consists of a cationic unit $[Ag(Hpz^{NO_2})_3]^+$ which is linked through a moderate hydrogen-bond N2–H2···O9 to the $PO_2F_2^-$ counteranion (Table 2), and an additional Hpz^{NO_2} molecule which is linked to the cationic unit through an additional hydrogen-bond N8–H8···N11 (Table 2).

In the cationic unit, the silver centre is three-coordinated to the pyridinic N-atoms of three pyrazole ligands, exhibiting a pseudo-C_3 axis passing through the metal atom. In this environment, the Ag–N distances (Table 1) are again in the range observed for related compounds [6,9–11b,19,21], and they compare well with those found in compound **6**. However, the N–Ag–N angles deviate from the ideal value of 120°, this fact being attributed to the

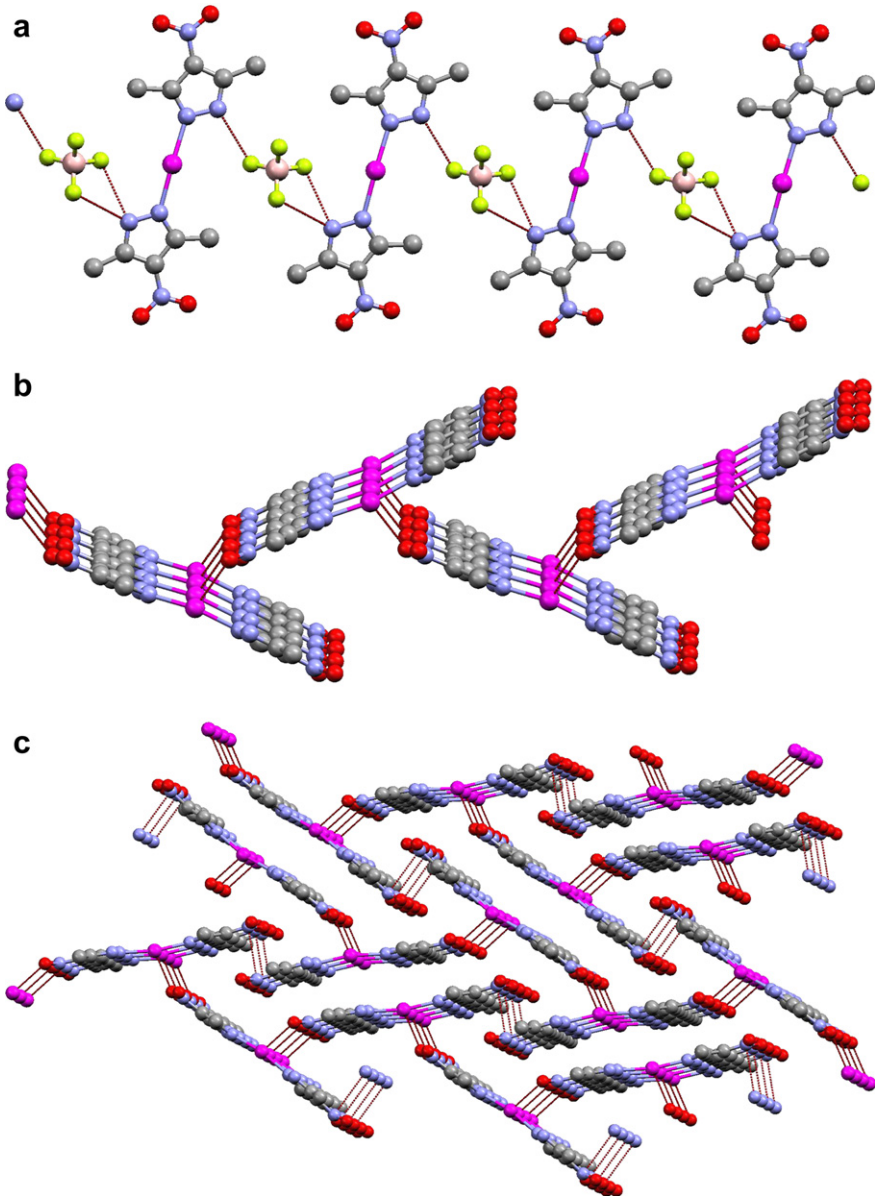

Fig. 4. (a) View of the 1D distribution along the *a* axis for **5** showing the hydrogen-bonds. (b) View of the two-dimensional network in the *ab* plane for **5** showing the Ag···O interactions. The counteranions are omitted for clarity. (c) View of the 3D network for **5** showing the Ag···O and π···π (NO_2···NO_2) interactions. The counteranions are omitted for clarity.

presence of the fourth non-coordinated pyrazole. The three planes of the coordinated pyrazoles are twisted each to other with dihedral angles of 72.9(3)°, 61.9(2)° and 74.7(3)°. The ring of the non-coordinated pyrazole lies almost parallel to one of the coordinated pyrazoles (dihedral angle of 4.9(2)°), but twisted with respect to the other ones (dihedral angles of 66.6(2)° and 74.8(2)°).

The hydrogen-bond between the $PO_2F_2^-$ counteranion and the cationic unit produces an approach of the silver centre to one of the oxygen atoms giving rise to a coordinative Ag···O9 interaction of 2.873(8) Å.

The non-coordinated pyrazole still has the possibility to perform a new hydrogen-bond which is established through the O10 atom from the $PO_2F_2^-$ counteranion from the closest unit (Table 2). In this way, the hydrogen-bonds define chains which are propagated through the *a* axis (Fig. 10a).

Neighbouring chains exhibit opposite orientations, giving rise to an approach of those pyrazoles not implicated in previous hydrogen-bonds. It produces a new hydrogen-bond N2–H2···O5 (Table 2), so generating a double chain (Fig. 10b).

In summary, the crystal packing (Fig. 10c) defines a 1D network produced by double chains formed through moderate hydrogen-bonds, without additional interactions among them.

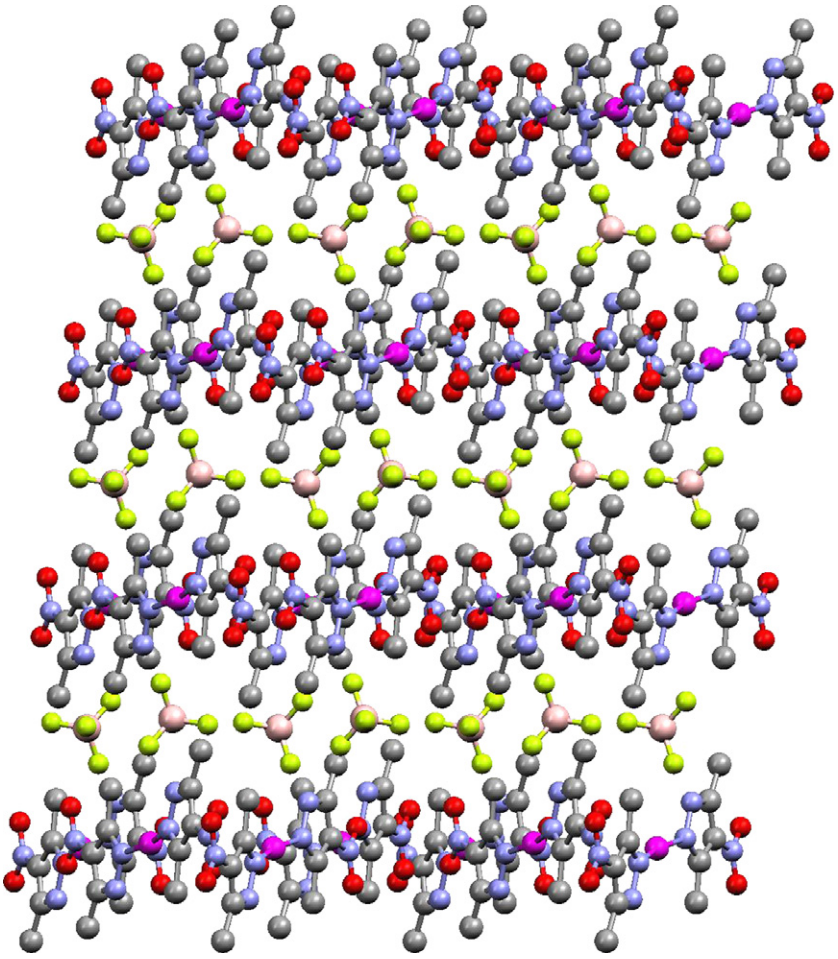

Fig. 5. View of the 3D network for **5** through the *b* axis.

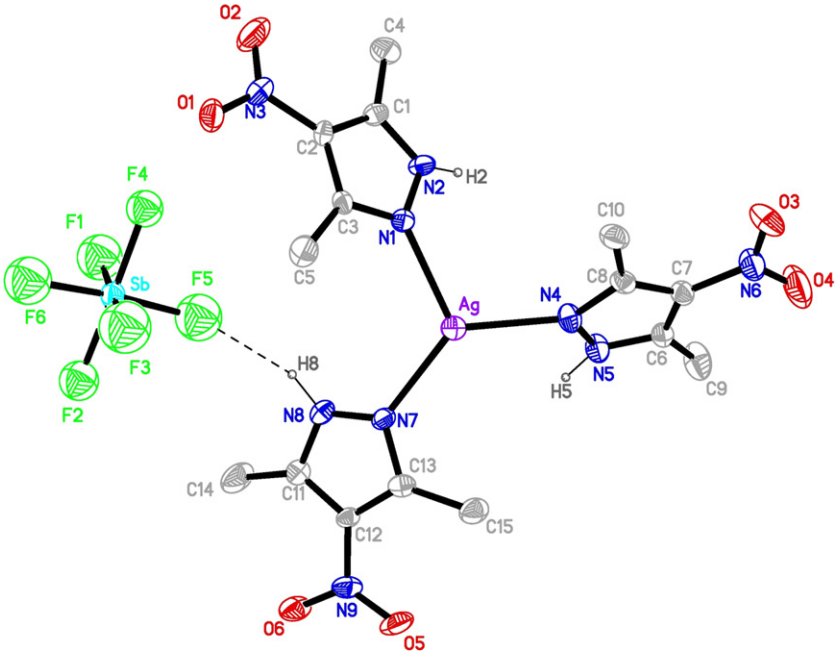

Fig. 6. A ORTEP view of $[Ag(Hpz^{NO_2})_3][SbF_6]$ (**6**), showing the numbering atom. Hydrogen atoms, except H2, H5 and H8, have been omitted for clarity. The thermal ellipsoids are at 25% probability level.

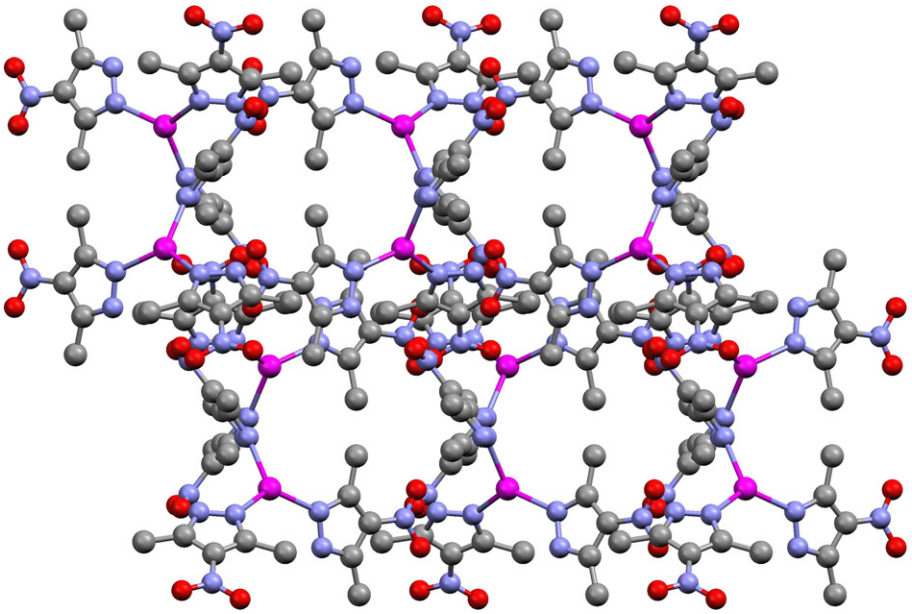

Fig. 7. View of the cationic sub-network of **6**.

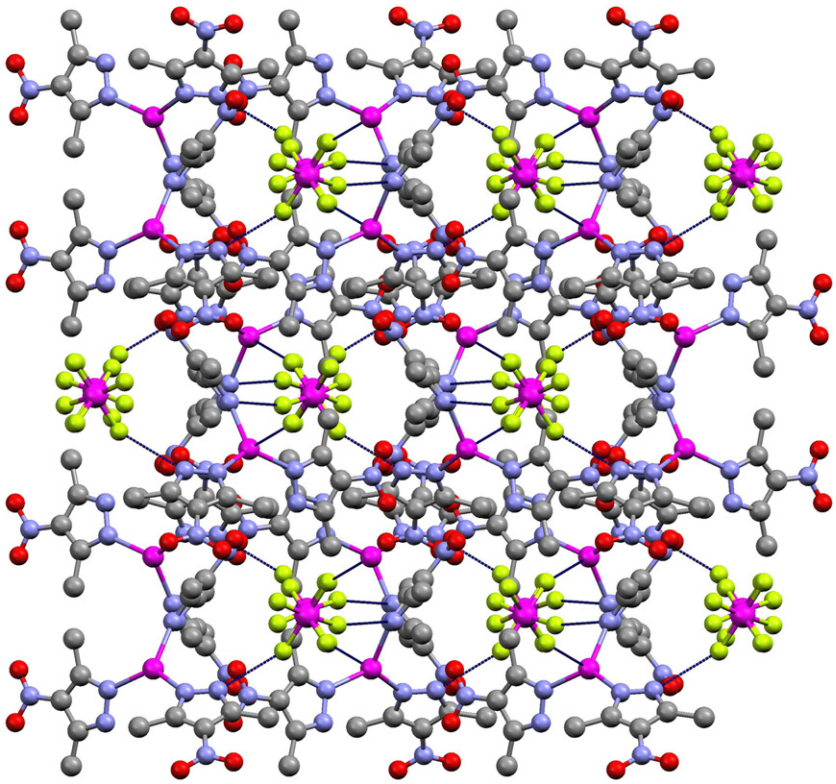

Fig. 8. View of the 3D structure for **6**, showing the occupancy of the channels of the cationic sub-network by the counteranions SbF_6^- and the Ag···F and N–H···F interactions.

3. Experimental

3.1. Materials and instrumentation

All commercial reagents were used as supplied. The ligand 3,5-dimethyl-4-nitropyrazole (Hpz^{NO_2}) was prepared by the literature procedures [23].

Elemental analyses for carbon, hydrogen and nitrogen were carried out by the Microanalytical Service of Complutense University. IR spectra were recorded on a FTIR ThermoNicolet 200 spectrophotometer with samples as KBr pellets in the 4000–400 cm^{-1} region.

^1H NMR spectra were performed on a Bruker AC200 (200.13 MHz) and $^{31}P\{^1H\}$ NMR spectrum was recorded

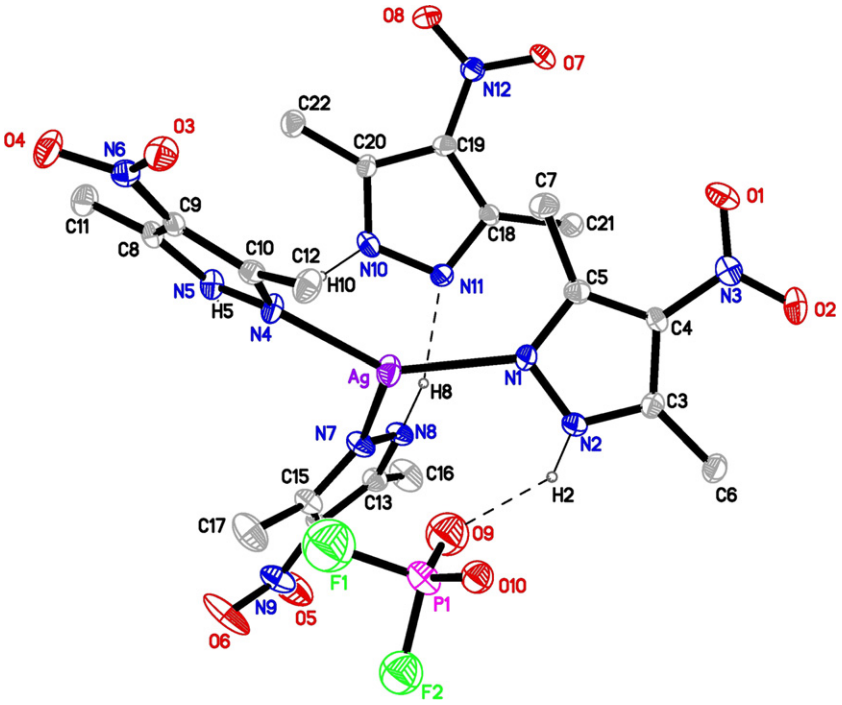

Fig. 9. A ORTEP view of $[Ag(Hpz^{NO_2})_3][PO_2F_2] \cdot Hpz^{NO_2}$ (**7**), showing the numbering atom. Hydrogen atoms, except H2, H5, H8 and H10, have been omitted for clarity. The thermal ellipsoids are at 20% probability level.

on a Bruker DPX-300 (121.49 MHz) of the NMR Service of Complutense University, from solutions in $CDCl_3$ at room temperature. Dilution and variable temperature ^1H NMR experiments were carried out on a Bruker Avance 500-AV (500.13 MHz) of the NMR Service of Complutense University. Chemical shifts δ(H) (±0.01 ppm) are listed relative to TMS using the signal of the deuterated solvent as reference (7.26 ppm), and δ(P) (±0.3 ppm) relative to 85% H_3PO_4. Coupling constants (*J*) are in Hz.

3.2. Synthetic methods

3.2.1. Synthesis of $[Ag(Hpz^{NO_2})_2][BF_4]$ (5)

This compounds was prepared as described previously [6]. Adequate single crystals were grown from dichloromethane/hexane solutions.

3.2.2. Synthesis of $[Ag(Hpz^{NO_2})_3][SbF_6]$ (6)

$AgSbF_6$ (125.0 mg, 0.363 mmol) was added under nitrogen atmosphere to a solution of Hpz^{NO_2} (154.0 mg, 1.091 mmol) in dry THF (20 mL). The resulting mixture was stirred for 24 h in the absence of light. Then it was filtered through a plug of Celite and the obtained colourless clear filtrate was evaporated to dryness, giving rise to an oil from which a white solid was isolated after the addition of dichloromethane and pentane. This product was crystallised by diffusion of hexane into a dichloromethane solution. Yield: 60%. $C_{15}H_{21}F_6N_9O_6SbAg$ (767.00): Calc. C, 23.5; H, 2.8; N, 16.4. Found C, 23.4; H, 2.8; N, 16.3%. IR (KBr, cm^{-1}): 3360–2700 ν(N–H) + ν(C–H), 1600 ν(C–N) + ν(C–C), 1509 $\nu_{as}(NO_2)$, 1365 $\nu_s(NO_2)$, 665 $\nu(SbF_6)$. ^1H NMR ($CDCl_3$, ppm): 2.73 (s, CH_3).

3.2.3. Synthesis of $[Ag(Hpz^{NO_2})_3][PO_2F_2] \cdot Hpz^{NO_2}$ (7)

This compound was prepared in a similar way to **6**, from $AgPF_6$ (130 mg, 0.514 mmol) and Hpz^{NO_2} (218.5 mg, 1.542 mmol). Crystals were obtained by slow diffusion of hexane into a dichloromethane solution of the compound. Yield: 45%. $C_{20}H_{28}F_2N_{12}O_{10}PAg$ (773.36): Calc. C, 31.1; H, 3.7; N 21.7. Found: C, 30.9; H, 3.6; N, 21.5%. IR (KBr, cm^{-1}): 3210–2750 ν(N–H) + ν(C–H), 1593 ν(C–N) + ν(C–C), 1509 $\nu_{as}(NO_2)$, 1365 $\nu_s(NO_2)$, 1295 ν(PO), 833 ν(PF) overlapped with pyrazole absorptions. ^1H NMR ($CDCl_3$, ppm): 2.70 (s, CH_3). $^{31}P\{^1H\}$ NMR ($CDCl_3$, ppm): −15.5 (t, $^1J_{P-F} = 959$ Hz).

3.3. X-ray structure determinations of 5–7

Colourless prismatic single crystals of **5**–**7** suitable for X-ray diffraction experiments were successfully grown by slow diffusion of hexane into a dichloromethane solution of each compound. Data collections were carried out at room temperature on a Bruker Smart CCD diffractometer, with graphite-monochromated Mo K_α radiation ($\lambda = 0.71073$ Å), operating at 50 kV and 25 mA. In all cases data were collected over a hemisphere of the reciprocal space by combination of the three exposure sets. Each frame exposure time was of 20 s, covering 0.3° in ω. The first 100 frames were recollected at the end of the data collection to monitor crystal decay. No appreciable drop in the

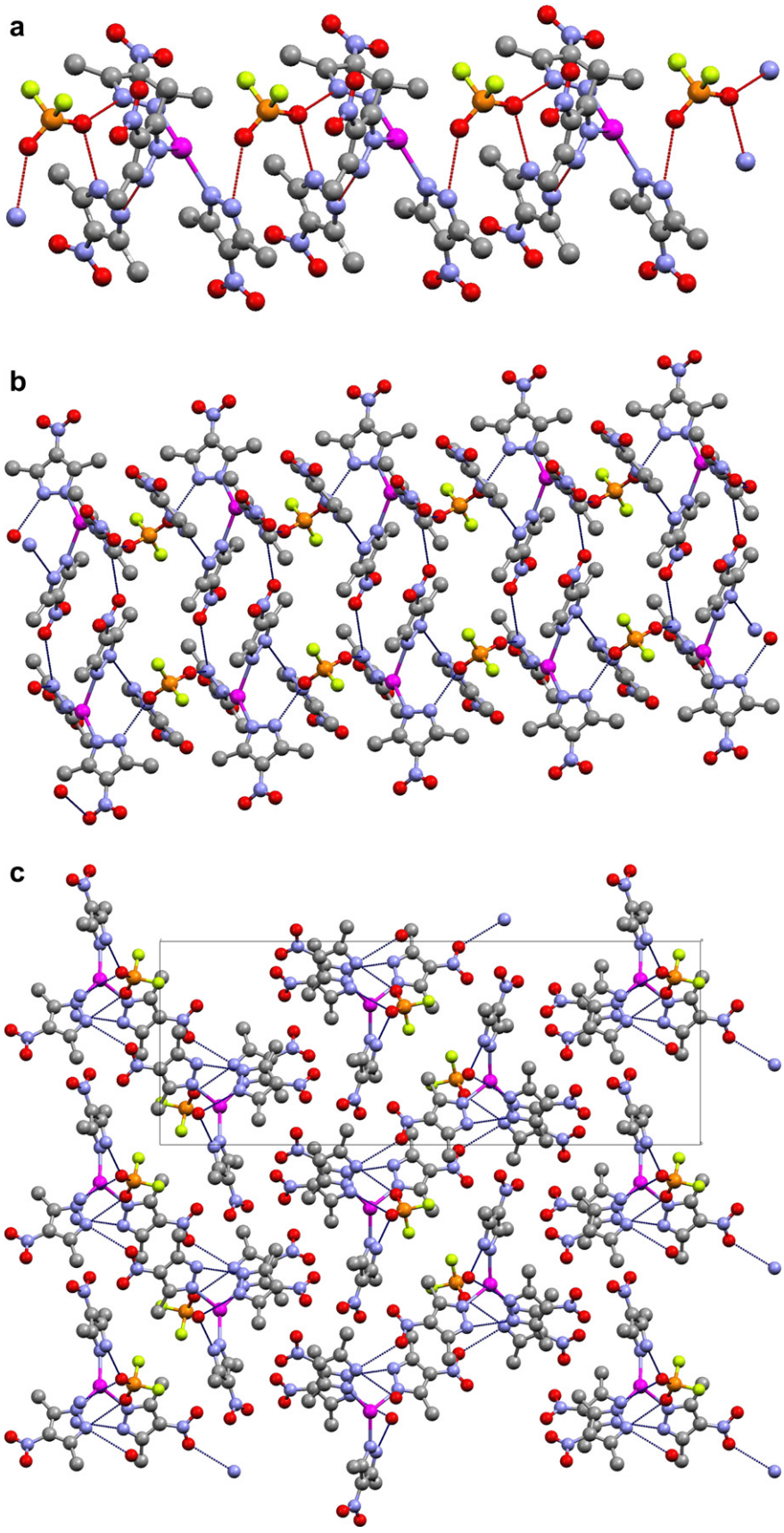

Fig. 10. (a) View of the chain in **7** along the *a* axis, showing the hydrogen-bonds. (b) View of the double chain in **7**, showing the hydrogen-bonds. (c) Crystal packing of **7** in which the double chains are propagated along the *a* axis.

Table 3
Crystal and refinement data for **5**–**7**

	5	**6**	**7**
Empirical formula	$C_{10}H_{14}BF_4N_6O_4Ag$	$C_{15}H_{21}F_6N_9O_6SbAg$	$C_{20}H_{28}F_2N_{12}O_{10}PAg$
Formula weight	476.95	767.03	773.38
Crystal system	Monoclinic	Orthorhombic	Monoclinic
Space group	$P2_1/c$	$Pbca$	$P2_1/c$
a (Å)	8.6968(6)	17.216(1)	8.400(1)
b (Å)	15.064(1)	17.287(1)	11.811(2)
c (Å)	13.532(1)	17.442(1)	31.507(4)
β (°)	96.392(1)		95.536(3)
V (Å^3)	1761.8(2)	5190.8(6)	3111.2(7)
Z	4	8	4
T (K)	296(2)	296(2)	296(2)
$F(000)$	944	2992	1568
ρ_{calc} (g cm^{-3})	1.798	1.963	1.651
μ (mm^{-1})	1.213	1.887	0.782
Scan technique	ω and φ	ω and φ	ω and φ
Data collected	$(-11,-19,-17)$–$(11,19,17)$	$(-20,-20,-17)$–$(20,20,20)$	$(-9,-11,-37)$–$(9,14,37)$
θ Range (°)	3.03–29.09	2.04–25.00	1.30–25.00
Reflections collected	16475	38022	23354
Independent reflections	4243 ($R_{int} = 0.0612$)	4573 ($R_{int} = 0.1045$)	5350 ($R_{int} = 0.0660$)
Completeness to maximum θ (%)	89.9	100.0	97.9
Data/restraints/parameters	4243/0/241	4573/0/317	5350/0/407
Observed reflections [$I > 2\sigma(I)$]	2027	2457	3031
Goodness-of-fit (F^2)	1.023	0.984	1.005
R[a]	0.0426	0.0659	0.0599
Rw_F^2[b]	0.1370	0.2261	0.2002
Largest residual peak (e Å^{-3})	0.690	2.117	1.300

[a] $\sum[|F_o| - |F_c|]/\sum|F_o|$.
[b] $\{\sum[w(F_o^2 - F_c^2)^2]/\sum[w(F_o^2)^2]\}^{1/2}$.

intensities of standard reflections was observed. A summary of the fundamental crystal data and refinement data are given in Table 3.

The structures were solved by direct methods and conventional Fourier techniques. The refinement was done by full-matrix least-squares on F^2 (SHELXS-97) [24]. Anisotropic parameters were used in the last cycles of refinement for all non-hydrogen atoms with some exceptions. For **6** and **7**, the fluorine and oxygen atoms of the SbF_6^- and $PO_2F_2^-$ groups, respectively, have been refined isotropically. Hydrogen atoms bonded to the nitrogen atoms have been located in a Fourier synthesis, included and their coordinates fixed or refined. The remaining hydrogen atoms were included in calculated positions and refined as riding on their respective carbon atoms and the thermal parameters related to the bonded atoms. The largest residual peaks in the difference map (Table 3) for **6** and **7** were found in the vicinity of the fluorine atoms of the SbF_6^- group and the oxygen atoms of the $PO_2F_2^-$ group, respectively. Final $R(R_w)$ values were 0.0426(0.1370), 0.0659(0.2261) and 0.0599(0.2002) for **5**, **6** and **7**, respectively.

4. Concluding remarks

In this work, new ionic silver(I) pyrazole-based complexes have been designed to perform supramolecular assemblies, which were mainly obtained by an anion-directed process. In particular, in the two-coordinated complexes $[Ag(Hpz^{NO_2})_2][AX_n]$ the influence of the counteranion has been proved to be determinant in the final network. The *cis* NH,NH-geometry, established when the $CF_3SO_3^-$ counteranion was present (**4**), has been changed by the smaller and uncoordinative BF_4^- anion to a *trans* orientation of the pyrazole groups (**5**), which is involved in the formation of polymeric 1D chains through moderate hydrogen-bonds with the counteranions. The role of the NO_2 substituent on the pyrazole ligand as linker of those chains was also confirmed in defining the extended supramolecular structure of the solid.

The X-ray structure of the compound $[Ag(Hpz^{NO_2})_3][SbF_6]$ (**6**) has shown how the octahedral anions SbF_6^- are encapsulated at the centre of cavities of the cationic assembly, providing evidence of the coordinative and hydrogen-bonding interactions between the F atoms of the anion and the metal centre and the NH-pyrazolic group, respectively. Once again, the anion plays an important role yielding to 3D supramolecular open networks, and it opens new expectatives to pursue this kind of structures.

The difference observed in the packing of **6** and **7** can be attributed to the presence of the pyrazole of crystallisation in **7**, which avoids the formation of channels and thus reducing the dimensionality of the molecular arrangement.

The results of this work indicate that the efficient selection of counteranions, stoichiometry and substituents at

the pyrazole are determinant for required supramolecular networks of metal pyrazole-based complexes.

5. Supplementary material

CCDC 638858, 638859 and 638860 contain the supplementary crystallographic data for **5**, **6** and **7**. These data can be obtained free of charge via http://www.ccdc.cam.ac.uk/conts/retrieving.html, or from the Cambridge Crystallographic Data Centre, 12 Union Road, Cambridge CB2 1EZ, UK; fax: (+44) 1223-336-033; or e-mail: deposit@ccdc.cam.ac.uk.

Acknowledgements

Financial support from the DGI of the Ministerio de Educación y Ciencia (Project No. BQU2003-07343) and Universidad Complutense (UCM2005-910300) is gratefully acknowledged.

References

[1] B.-H. Ye, M.-L. Tong, X.-M. Chen, Coord. Chem. Rev. 249 (2005) 545.
[2] (a) A.M. Beatty, Coord. Chem. Rev. 246 (2003) 131;
(b) J.C. McDonald, G.M. Whitesides, Chem. Rev. 94 (1994) 2383;
(c) S. Subramaniam, M.J. Zaworotko, Coord. Chem. Rev. 137 (1994) 357;
(d) D. Braga, F. Grepioni, G.R. Desiraju, Chem. Rev. 98 (1998) 1375;
(e) D. Braga, J. Chem. Soc., Dalton Trans. (2000) 3705;
(f) A.M. Beatty, CrystEngComm. 3 (2001) 243.
[3] (a) J.M. Lehn, Supramolecular Chemistry, VCH, New York, 1995;
(b) J.W. Steed, J.L. Atwood, Supramolecular Chemistry, Wiley, New York, 2000;
(c) M. Eddaoudi, J. Kim, N. Rosi, D. Vodak, J. Wachter, M. O'Keefe, O.M. Yaghi, Science 295 (2002) 469;
(d) B.J. Holliday, C.A. Mirkin, Angew. Chem., Int. Ed. 40 (2001) 2022;
(e) P.M. Hagrman, D. Hagrman, J. Zubieta, Angew. Chem., Int. Ed. 38 (1999) 2638;
(f) O.M. Yaghi, H. Li, J. Am. Chem. Soc. 117 (1995) 10401;
(g) H.K. Chae, D.Y. Siberio-Perez, J. Kim, Y. Go, M. Eddaoudi, A.J. Matzger, M. O'Keefe, O.M. Yaghi, Nature 427 (2004) 523;
(h) G.J. Halder, C.J. Kepert, B. Moubaraki, K.S. Murray, J.D. Cashion, Science 298 (2002) 1762;
(i) B. Moulton, M.J. Zaworotko, Chem. Rev. 101 (2001) 1629;
(j) S.L. James, Chem. Soc. Rev. 32 (2003) 276;
(k) X.-H. Bu, M.-L. Tong, H.-C. Chang, S. Kitagawa, S.R. Batten, Angew. Chem., Int. Ed. 43 (2004) 192;
(l) B. Chen, N.W. Ockwig, A.R. Millward, D.S. Contreras, O.M. Yaghi, Angew. Chem., Int. Ed. 44 (2005) 4745;
(m) J.L.C. Rowsell, O.M. Yaghi, Angew. Chem., Int. Ed. 44 (2005) 4670;
(n) C. Janiak, Dalton Trans. (2003) 2781.
[4] (a) G.R. Desiraju, T. Steiner, The Weak Hydrogen Bond in Structural Chemistry and Biology, Oxford University Press, Oxford, 1999;
(b) G.R. Desiraju, J. Chem. Soc., Dalton Trans. (2000) 3745;
(c) C. Janiak, T.B. Scharmann, Polyhedron 22 (2003) 1123;
(d) T. Steiner, Angew. Chem., Int. Ed. 41 (2002) 48;
(e) A. Nangia, CrystEngComm. 4 (2002) 93;
(f) G.R. Desiraju, Acc. Chem. Res. 29 (1996) 441;
(g) T. Steiner, New. J. Chem. (1998) 1099;
(h) T. Steiner, Chem. Commun. (1997) 727;
(i) G.R. Desiraju, Chem. Commun. (2005) 2995.
[5] R.M. Claramunt, P. Cornago, M. Cano, J.V. Heras, M.L. Gallego, E. Pinilla, M.R. Torres, Eur. J. Inorg. Chem. (2003) 2693.
[6] M.L. Gallego, P. Ovejero, M. Cano, J.V. Heras, J.A. Campo, E. Pinilla, M.R. Torres, Eur. J. Inorg. Chem. (2004) 3089.
[7] M. Cano, J.V. Heras, M.L. Gallego, J. Perles, C. Ruiz-Valero, E. Pinilla, M.R. Torres, Helv. Chim. Acta 86 (2003) 3194.
[8] M.L. Gallego, M. Cano, J.A. Campo, J.V. Heras, E. Pinilla, M.R. Torres, Helv. Chim. Acta 88 (2005) 2433.
[9] H. Schmidbaur, A. Mair, G. Müller, J. Kachmann, S. Gamper, Z. Naturfosch. B 46 (1991) 912.
[10] A.A. Mohamed, J.P. Fackler Jr., Acta Crystallogr., Sect. C 58 (2002) m228.
[11] (a) T. Wu, R. Zhou, D. Li, Inorg. Chem. Commun. 9 (2006) 341;
(b) M. Munakata, M. Wen, Y. Suenaga, T. Kuroda-Sowa, M. Maekawa, M. Anahata, Polyhedron 20 (2001) 2037;
(c) M. Munakata, J. Han, A. Nabei, T. Kuroda-Sowa, M. Maekawa, Y. Suenaga, N. Gunjima, Inorg. Chim. Acta 359 (2006) 4281;
(d) Y.T. Wang, Y.L. Wang, J.G. Wang, Y.T. Fan, Acta Crystallogr., Sect. E 62 (2006) m1927;
(e) R.H. Wang, M.C. Hong, J.H. Luo, F.L. Jiang, L. Han, Z.Z. Lin, R. Cao, Inorg. Chim. Acta 357 (2004) 103.
[12] (a) V.R. Thalladi, S. Brasselet, D. Bläser, R. Boose, J. Zyss, A. Nangia, G.R. Desiraju, Chem. Commun. (1997) 1841;
(b) V.R. Thalladi, S. Brasselet, H.C. Weiss, D. Bläser, A.K. Katz, H.L. Carrell, R. Boose, J. Zyss, A. Nangia, G.R. Desiraju, J. Am. Chem. Soc. 120 (1998) 2563.
[13] K. Nakamoto, Infrared and Raman Spectra of Inorganic and Coordination Compounds, fourth ed., Wiley, New York, 1986.
[14] R. Fernández-Galán, B.R. Manzano, A. Otero, M. Lanfranchi, M.A. Pellinghelli, Inorg. Chem. 33 (1994) 2309.
[15] (a) J. Barberá, C. Cativiela, J.L. Serrano, M.M. Zurbano, Liq. Cryst. 11 (1992) 887;
(b) M.C. Torralba, M. Cano, J.A. Campo, J.V. Heras, E. Pinilla, M.R. Torres, J. Organomet. Chem. 633 (2001) 91;
(c) M.C. Torralba, M. Cano, J.A. Campo, J.V. Heras, E. Pinilla, M.R. Torres, J. Organomet. Chem. 654 (2002) 150;
(d) M.C. Torralba, M. Cano, J.A. Campo, J.V. Heras, E. Pinilla, M.R. Torres, Inorg. Chem. Commun. 5 (2002) 887.
[16] C. Foces-Foces, F.H. Cano, J. Elguero, Gazz. Chim. Ital. 123 (1993) 477.
[17] (a) M. Cano, J.V. Heras, M. Maeso, M. Alvaro, R. Fernández, E. Pinilla, J.A. Campo, A. Monge, J. Organomet. Chem. 534 (1997) 159;
(b) M. Cano, J.A. Campo, J.V. Heras, J. Lafuente, C. Rivas, E. Pinilla, Polyhedron 14 (1995) 1139.
[18] L. Chen, M.A. Khan, G.B. Richter-Addo, Inorg. Chem. 37 (1998) 533.
[19] (a) I. Boldog, E.B. Rusanov, A.N. Chernega, J. Sieler, K.V. Domasevitch, Polyhedron 20 (2001) 887;
(b) D.L. Reger, R.F. Semeniuc, M.D. Smith, Inorg. Chem. 40 (2001) 6545.
[20] (a) D.C. Zhang, Z.H. Fei, T.Z. Zhang, Y.Q. Zhang, K.B. Yu, Acta Crystallogr., Sect. C 55 (1999) 102;
(b) M. Hörner, I.C. Casagrande, H. Fenner, J. Daniels, J. Beck, Acta Crystallogr., Sect. C 59 (2003) m424;
(c) M. Hörner, L. Bresolin, J. Bordinhao, E. Hartmann, J. Strähle, Acta Crystallogr., Sect. C 59 (2003) o426.
[21] (a) M.L. Gallego, M. Cano, J.A. Campo, J.V. Heras, E. Pinilla, M.R. Torres, P. Cornago, R.M. Claramunt, Eur. J. Inorg. Chem. (2005) 4370;
(b) L. Carlucci, G. Ciani, D.M. Prosperio, A. Sironi, J. Am. Chem. Soc. 117 (1995) 4562;
(c) D. Venkataraman, S. Lee, J.S. Moore, P. Zhang, K.A. Hirsch, G.B. Gardner, A.C. Covey, C.L. Prentice, Chem. Mater. 8 (1996) 2030;

(d) L. Carlucci, G. Ciani, D.M. Proserpio, A. Sironi, Inorg. Chem. 34 (1995) 5698;
(e) L. Carlucci, G. Ciani, D.M. Proserpio, A. Sironi, Angew. Chem., Int. Ed. 34 (1995) 1895;
(f) D.L. Reger, R.F. Semeniuc, M.D. Smith, Inorg. Chem. Commun. 5 (2002) 278;
(g) C.-J. Lin, W.-S. Hwang, M.Y. Chiang, Polyhedron 20 (2001) 3275.
[22] N. Gimeno, R. Vilar, Coord. Chem. Rev. 250 (2006) 3161.
[23] G.T. Morgan, I. Ackerman, J. Chem. Soc. (1923) 1308.
[24] G.M. Sheldrick, SHELXL97, Program for Refinement of Crystal Structure, University of Göttingen, Göttingen, Germany, 1997.